McPherron and Chu *Geosci. Lett.* (2016) 3:12
DOI 10.1186/s40562-016-0044-5

Geoscience Letters

RESEARCH LETTER

Open Access

Relation of the auroral substorm to the substorm current wedge

Robert L. McPherron* and Xiangning Chu

Abstract

The auroral substorm is an organized sequence of events seen in the aurora near midnight. It is a manifestation of the magnetospheric substorm which is a disturbance of the magnetosphere brought about by the solar wind transfer of magnetic flux from the dayside to the tail lobes and its return through the plasma sheet to the dayside. The most dramatic feature of the auroral substorm is the sudden brightening and poleward expansion of the aurora. Intimately associated with this expansion is a westward electrical current flowing across the bulge of expanding aurora. This current is fed by a downward field-aligned current (FAC) at its eastern edge and an upward current at its western edge. This current system is called the substorm current wedge (SCW). The SCW forms within a minute of auroral expansion. FAC are created by pressure gradients and field line bending from shears in plasma flow. Both of these are the result of pileup and diversion of plasma flows in the near-earth plasma sheet. The origins of these flows are reconnection sites further back in the tail. The auroral expansion can be explained by a combination of a change in field line mapping caused by the substorm current wedge and a tailward growth of the outer edge of the pileup region. We illustrate this scenario with a complex substorm and discuss some of the problems associated with this interpretation.

Keywords: Auroral substorm, Magnetospheric substorm, Auroral expansion, Auroral bulge, Polar magnetic substorm, Westward electrojet, Substorm current wedge, Midlatitude positive bay index

Background

The word "substorm" first appeared in a review of magnetic storms by Chapman (1962). "Thus his polar storms I call polar substorms, and denote them and their currents by DP." The association of polar substorms, and the justification of the use of the term substorm, was further developed in three papers (Akasofu et al. 1963; Akasofu and Chapman 1963a, b). The development of the aurora in association with the polar substorm was described by Akasofu (1964) and named the auroral substorm. Subsequently, the relation of the polar substorm and the westward electrojet that it creates to the auroral substorm was described by Akasofu et al. (1965).

The evolution of the substorm concept to include phenomena outside the ionosphere began with a paper by Jelly and Brice (1967) which noted that "…auroral precipitation is not a spatially isolated phenomenon, but is intimately connected with large-scale processes that occupy a substantial part of the magnetosphere." Consequently, they suggested that a new term "elementary magnetospheric substorm" be introduced to describe this behavior. One author of this paper (RLM) heard the original talk and later he and his colleagues discussed the terminology with one of its authors (NB). We argued that the term was too complex and that a more appropriate term was "magnetospheric substorm." The justification for this was first made in conference proceedings (McPherron 1967) where we concluded "In order to generalize the concept of the auroral substorm to include the world-wide disturbance characteristics and to emphasize the importance of the magnetosphere in auroral zone observations, we suggest a new terminology: magnetospheric substorm." This idea was published later in Coroniti et al. (1968) where we said. "…It is clear, then, that the auroral substorm is part of a worldwide disturbance, and that it is the dynamical processes occurring throughout the magnetosphere that determine the local-time characteristics of the substorm." Observational support for this

*Correspondence: rmcpherron@igpp.ucla.edu
Department of Earth, Planetary and Space Sciences, University of California Los Angels, Los Angeles, CA 90005-1567, USA

conclusion was provided in two other papers (McPherron et al. 1968; Parks et al. 1968); Brice (1967) continued to advocate for the longer name but the shorter name became the standard terminology.

The original auroral substorm model consisted of two phases: the expansive phase (10–30 min) and the recovery phase (~2 h). The onset of the substorm was taken as the start of the expansive phase which begins in a quiet arc near midnight and includes a sudden brightening and rapid poleward expansion. The recovery phase begins when the expanding aurora reaches its highest latitude and begins to fade. Akasofu noted that it was not uncommon for a brightening to occur with only a weak expansion. He called these "pseudo breakups." The substorm sequence was modified in 1970 by the addition of a growth phase prior to the onset of the expansion phase (McPherron 1970). For many years, the existence of a growth phase was highly controversial (Mozer 1973; Vasyliunas and Wolf 1973; Cowley 1982). However, as more data became available, its existence before isolated substorms became well established. Many years later, it was found that intensifications of the aurora could also occur at the poleward boundary of the auroral oval De La Beaujardiere et al. (1991, 1994). Subsequently, these poleward boundary intensifications (PBI) were associated with fast flows in the tail and equatorward moving auroral streamers (Lyons et al. 1999; Sergeev et al. 1999).

The typical substorm is usually more complex than a succession of three simple phases Rostoker et al. (1980, 1987). During the growth phase, there may be several pseudo breakups prior to the onset of the expansion phase. During the expansion phase, there are often multiple steps with each one corresponding to further poleward motion of the aurora. When the aurora reaches, high latitude PBI begin and auroral streamers are seen. When no auroral data are available, it is often difficult to determine from other indicators when the auroral expansion occurs and even with such data it is easy to confuse a brightening or pseudo breakup with the main onset. In the absence of auroral data, ground magnetometers are used to time the substorm expansion onset. The first of these was the sudden onset of a negative bay (a rapid decrease) in the horizontal magnetic field (H) at an auroral zone magnetometer near midnight (Akasofu et al. 1965). An association between negative bays in the auroral zone and positive bays at midlatitudes was noted by Akasofu and Meng (1969) and first interpreted as an ionospheric return current from the westward electrojet. McPherron (1972) suggested that the cause of the midlatitude positive bay is a diversion of the tail current through the midnight ionosphere as illustrated in Fig. 1 (McPherron et al. 1973; Horning et al. 1974). The possibility of a three-dimensional current system had been considered by a number of authors about this time as reviewed in Fukushima and Kamide (1973), but no one could prove that the system really existed using only ground observations. McPherron (1972) showed that the perturbations at synchronous orbit had the same sign as seen on the ground at Honolulu implying that the current system was above or outside the spacecraft.

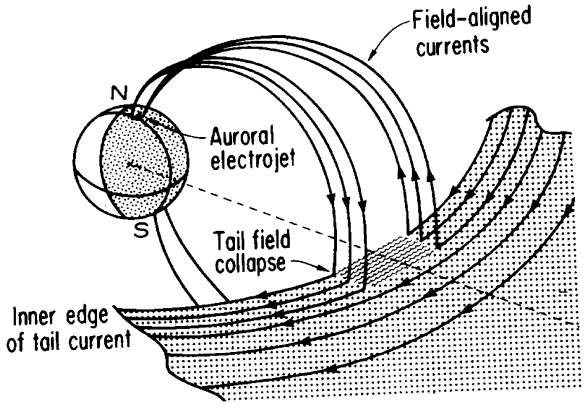

Fig. 1 The substorm current wedge diverts tail current through the ionosphere. A schematic representation of the substorm current wedge as originally envisioned (McPherron et al. 1973). At the *inner edge* of the plasma sheet tail current is diverted along field lines closing westward in the midnight ionosphere and returning to the tail from the westward surge. Previously stretched field lines collapse to a more dipolar configuration (dipolarization)

In the remainder of this paper, we illustrate the relation between the midlatitude positive bays and several other indicators of substorm onset and show why it is often so difficult to establish an accurate time sequence of events occurring during a substorm.

Methodology

A modern current wedge model is described in Chu et al. (2014). In this model, the current flows on realistic field lines rather than dipole lines, it uses sheet currents rather than line currents, it includes changes in partial and symmetric ring current, and it includes images of these currents beneath the earth. Midlatitude ground magnetometer data can then be inverted to obtain the parameters of the current wedge as a function of time throughout a substorm. To determine intervals suitable for inversion, we have developed a new magnetic index which we call the midlatitude positive bay index (MPB) (Chu et al. 2015a). The onset of a midlatitude positive bay is evident as rapid increase of the index from a background level to a higher value. We take the time of a sudden change in slope as the midlatitude onset.

In its most general application, the current wedge model has a large number of free parameters. In our

routine inversions, we set the radial distances of the partial and symmetric ring currents; the location of the up and down currents in the partial ring current, and the L-shell on which the field-aligned current of the wedge flows. Free parameters include the width of the upward and downward sheets, the local times of the center of these sheets, and the total current flowing in the wedge. This combination of fixed and free parameters is sufficient to obtain prediction efficiency at the end of the expansion phase as high as 95 % of the variance in the measured data. The inverted parameters reveal how the current wedge develops in both space and time.

Results

Case study

An example of the variation in the MPB index during a complex substorm is presented in Fig. 2, where five different indicators of substorm activity have been plotted. Panel (a) displays the optimum solar wind coupling function for AL (McPherron et al. 2015). Two intervals of moderate coupling occurred between 07:30 and 08:00 and 08:55–09:40 UT. Panel (b) shows the total luminosity recorded by three all sky imagers (ASI) across Canada (see legend). There were at least three major brightenings in the aurora between 7 and 11 UT, but only the last at 09:37 was correlated with other indictors of substorm onset. Panel (c) displays power in Pi 2 pulsations (period of 40–150 s) at the midlatitude station Fresno, CA. A weak Pi 2 occurred at about 07:40 UT and a stronger one at 08:30 both of which show no association with any major changes in other signals. A large increase in luminosity at 09:00 was associated with very weak midlatitude Pi 2, and with a moderate drop (negative bay) in the SuperMag SML index (Newell and Gjerloev 2011) plotted in panel (d). At 09:29, there was a short Pi 2 burst that was associated with a very weak drop in SML but no other indicator. Finally, 6 min later at 09:37 all three ASI observed a sudden increase in luminosity. At 09:37, there was a large drop in SML, followed by a major Pi 2 onset at 09:38:01, and finally in panel (e) a significant increase in the MPB index after 09:39. Subsequently, there may have been an intensification of the luminosity, Pi 2, and SML index, but the MPB index increased smoothly reaching a maximum just before 10 UT. We take the time 09:37–09:39 when all indicators show sudden changes as the main onset of a substorm expansion. Note in panel (d) in addition to SML we have also plotted the standard AL index (red) and the THEMIS AL (black). It is apparent that there are substantial differences in the three traces arising from the number of stations used. Similarly in panel (e), we have plotted results from two different algorithms for calculating the MPB index which exhibit slightly different behavior. Again the number of stations used is important as are the procedures for the elimination of other sources of magnetic variation.

This example makes clear how different observers might come to quite different conclusions concerning the sequence of events during a substorm. Other indicators of substorm onset not presented include the onset of auroral kilometric radiation (AKR), dipolarization of the magnetic field at synchronous orbit, dispersionless injection of energetic particles at synchronous orbit, extrema in the X and Z components of the lobe magnetic field, plasma sheet thinning, and fast earthward flows in the plasma sheet. In individual events, some phenomena are not seen or occur at slightly different times in the sequence. Only by statistical studies of a large number of substorms, is it possible to determine the average substorm sequence.

We have inverted the midlatitude magnetic data for this event with the results as shown in Fig. 3. Panel (a) displays the optimum coupling function (McPherron et al. 2015) and the universal coupling function (UCF) (Newell and Gjerloev 2011). These functions of solar wind variables are designed to be highly correlated with the AL index plotted in the second panel and are virtually identical. It can be seen that both began to increase about 08:55 reaching a steady value at 09:06. From 09:32 to 09:38, coupling briefly decreased. At 09:38, it sharply increased back to the original level and there was a major substorm expansion onset. One minute later, the current in the wedge plotted in panel (c) began to steadily increase reaching a maximum of 195,000 Amps at 09:54 (16 min duration). In the next 30 min, the current decayed to a value too weak for the midlatitude inversion to track. Panel (d) shows in blue the location of the center of the downward current in the wedge, and in red the center of the upward current. The initial locations are not reliable because of weak midlatitude perturbations but it appears that the initial wedge extended from -4 to $+2$ h local time. Thereafter, it expanded slowly to the east reaching $+4$ h local time. The upward current expanded westward more rapidly reaching dusk at the time of maximum current. After this time, the upward current appears to expand into the afternoon sector. The dashed black line is the local time of the GOES 11 spacecraft which was 40 min past midnight at the time of the main onset. The magnetic field parallel to the earth's rotation axis (Hp) is plotted in the bottom panel (e). At about 09:10, Hp began to decrease reaching a minimum at the time of the main onset. It remained constant until the end of the expansion phase at 09:54 when it began to recover, i.e., to return to a more dipolar configuration (dipolarization). At this time, it is likely that the east edge of the current wedge had moved beyond GOES 11 causing the field to dipolarize. We emphasize that in this case the onset of dipolarization was delayed relative to the main onset.

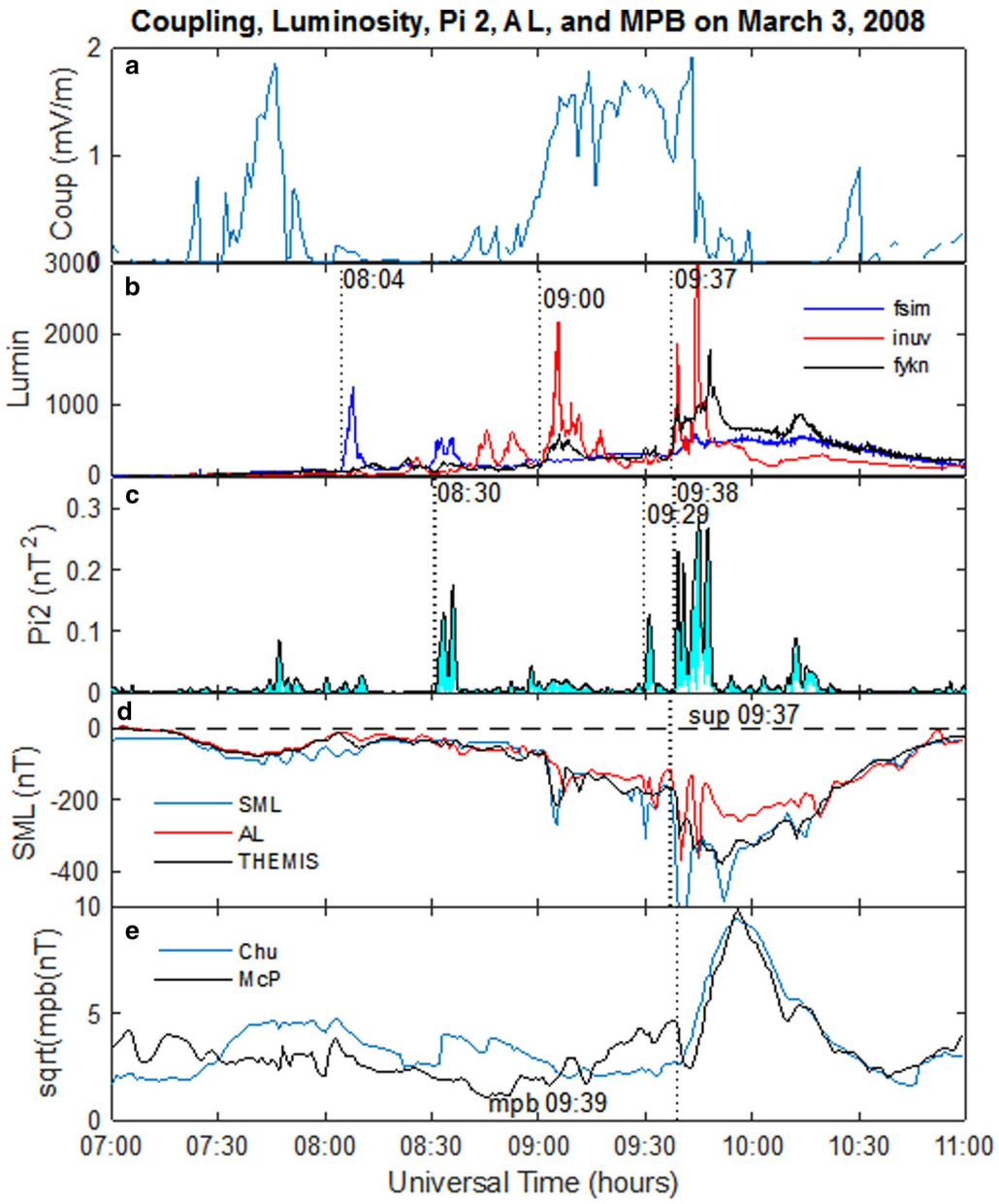

Fig. 2 Characteristic changes in different variables reveal substorm development. Solar wind coupling function (**a**), traces of auroral luminosity (**b**), Pi 2 pulsation power (**c**), SuperMag AL index (**d**), and the Midlatitude positive bay (MPB) index (**e**) are presented in successive panels for an event on March 3, 2008. *Vertical dotted lines* in each panel show onset times. Spikes in luminosity indicate intensification of the aurora. Peaks in Pi 2 power show waves communicating between the tail and ionosphere. Sudden drops in the SML index show enhancements of westward current beneath the aurora. A peak in the MPB index is produced by the growth and decay of the substorm current wedge

We have processed the auroral data from the three ASI instruments, as shown in Fig. 2, producing keograms (maps of luminosity along the central meridian of the instrument as a function of magnetic latitude and universal time). These maps are available in Additional file 1: Figure S1, Additional file 2: Figure S2 and Additional file 3: Figure S3. In each map, the vertical dashed lines correspond to the onset of plasma flows at either THEMIS D or E as described below. The Fort Simson keogram shows significant intensifications shortly after 8:04, 08:28, and 08:56 and weak ones after 08:17 and 09:38 UT. In this case, there is short delay between the onset of flows (white dashed lines) and the auroral intensification at fsim so we assume they could have been caused by the arrival

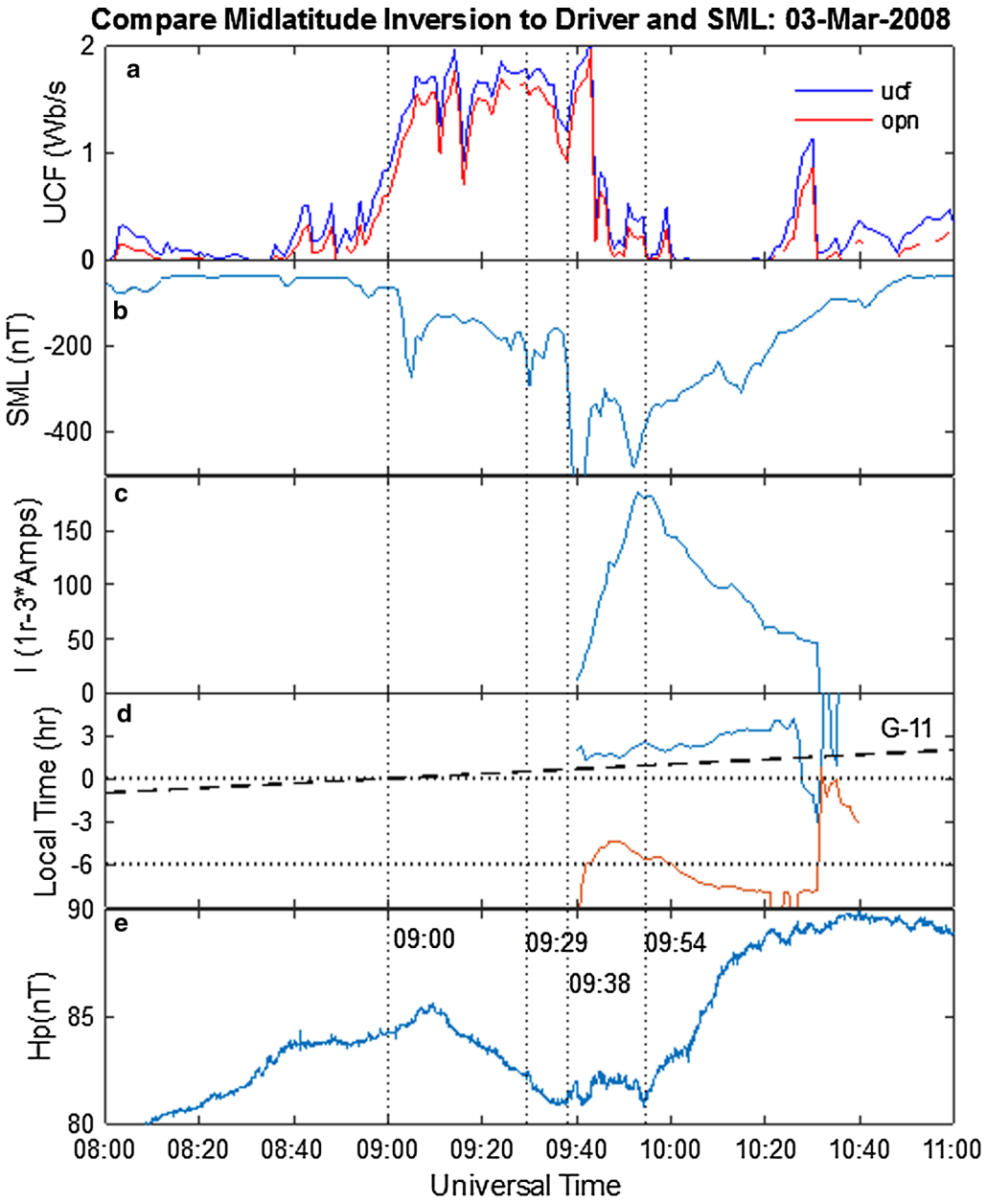

Fig. 3 Properties of a substorm current wedge on March 3, 2008 are displayed as a function of time. Panel **a** shows the universal coupling function (UCF) and the optimum function (opn) that drive the developments of auroral zone negative bays plotted in panel **b** and the growth of the current wedge *plotted* in panels **c** and **d**. Panel **c** displays the strength of the current as a function of time. The locations of the upward and downward currents are shown by *red* and *blue* traces in panel **d**. In this panel the *dashed line* shows the location of the GOES-11 spacecraft relative to the current wedge. The THEMIS spacecraft were near midnight along the *dotted line*. The bottom panel **e** displays the component of the magnetic field at GOES parallel to the earth's rotation axis (Hp)

of the flows. The aurora at Inuvik station further west was more active with equatorward moving forms at ~08:25, 08:40, and 08:50. An examination of an auroral mosaic contained in Additional file 4: File 1 demonstrates that these forms are actually east–west arcs becoming progressively brighter at lower latitudes. At 09:01:15, a quiet arc at 69.5° intensified and expanded poleward to 73°. The aurora moved equatorward after 09:04. Another brightening and poleward expansion began at 09:36:34 with equatorward moving forms at 09:41 and 09:43. None of these brightenings are closely associated with the onset of flow bursts. The last brightening began before the flow burst. Further west Fort Yukon observed weak auroral activity starting at 08:10 and lasting until 09:02 when there was

a sudden brightening and poleward expansion. A second major brightening began at 09:37 before the onset of a flow burst. Both intensifications appear to have been caused by westward traveling surges crossing the station.

In reality, the auroral activity is far more complex than suggested by the keograms. Justification of this statement can be found in Additional file 4: File 1. This compressed file contains 2401 gif images with the aurora projected onto a mosaic of northwestern North America every 3 s. The image sequence begins at 08:00:00 when only quiet arcs were present. At 08:04:09, the equatorward arc over Fort Simson began to brighten and 30 s later developed a sequence of bright spots on the poleward edge of the arc. This activation extended westward and several degrees poleward and then faded at 08:14:00. At 08:25, brightening of an auroral arc rapidly extended westward across Alaska. At 08:30 a breakup began in Western Canada but did not expand very far poleward. There was no negative bay and no midlatitude positive bay associated with this activation. At 09:01:30 another breakup began across Alaska with the formation of a westward surge. The equatorward motion seen at Inuvik after 09:11 appears to have been caused by westward motion of a complex loop in the aurora. The next breakup over Inuvik can be seen in the 09:36:00 image as a beaded arc well south of another arc. In the mosaic it can be seen that an equatorward moving streamer emerged from the brightened aurora at 09:38:30, and by 09:41:00 multiple streamers were simultaneously emerging from the poleward arc. At 10:07:30, a new beaded arc formed poleward of all other activity.

During this event, THEMIS D and E spacecraft were at local times between 23 and 24 at a distance of ~11 Re. In Additional file 5: Figure S4, we have plotted the locations of all spacecraft and the center of the current wedge field-aligned current sheets. The symbols "X" denote locations each hour from 7 to 11 UT. The left-pointing triangles show the spacecraft locations at the onsets of five flow bursts recorded by THEMIS D & E. The ion speed and magnetic field strength measured by these two spacecraft are plotted in Fig. 4 with the sign of THEMIS E data reversed. The start times of various events are shown by color-coded annotation in each panel. These times are difficult to measure to better than about 30 s because of fluctuations in the traces. Corresponding event times at the two spacecraft are generally less than a minute apart. It is apparent that each flow burst is associated with significant changes in the magnetic field. In Additional file 6: Figure S5 and Additional file 7: Figure S6 we have plotted the GSM components of the magnetic field measured by both spacecraft. At both D and E each flow burst carried northward magnetic field causing Bz to increase in a stepwise manner starting at about 4 nT and ending at 20 nT.

The THEMIS C spacecraft was also in the tail at $R \sim 15$ Re during this substorm as shown in Additional file 5: Figure S4. A plot of the field and flow recorded by this spacecraft is included in Additional file 8: Figure S7. Panel (a) presents the estimates of the thermal, magnetic, and total plasma pressure. The plot indicates that the two intervals of solar wind coupling caused the plasma sheet to thin twice leaving the spacecraft in the plasma sheet boundary layer. The first three flow bursts seen closer to the Earth by THEMIS D & E were not evident at C in the boundary layer as can be seen in panel (b). However, the 08:28 flow burst and auroral intensification at Fort Simson caused a rapid expansion of the plasma sheet so that at 08:33 THEMIS C observed the start of a 40-min interval of pulsing earthward flow. The 08:56 flow burst had little effect at C, despite a thicker plasma sheet but corresponded to the onset of the second interval of thinning. THEMIS C again moved into the boundary layer until the 09:37 major substorm onset caused a rapid expansion of the plasma sheet and a strong burst of earthward flow.

Discussion

To understand the relation between various phenomena and the time sequence of this substorm, we have created a time sequence table placed in Additional file 9: Table S1. Entries in this table have been derived from magnified versions of each variable using a graphics cursor. The values shown on some graphs may be somewhat different as they were derived from low-resolution plots. Ground magnetometer data and indices have 1-min resolution. Luminosity and keograms have 3 s resolution as do the THEMIS ion velocity and magnetic field traces. The table has been divided into several sections corresponding to different flow bursts seen by THEMIS spacecraft. Fundamental to our interpretation is the assumption that the arrival of a flow burst at 11 Re indicates magnetic reconnection further out in the tail somewhat earlier.

To understand what is driving this activity, we examined plots of the solar wind electric field and solar wind coupling functions. During the interval 07–11 UT, there were only two intervals of southward interplanetary magnetic field (IMF): 07:35–07:47 and 08:57–09:46 UT. In the first interval, there was a very weak negative bay (~−50 nT) from 0722 to 0812. At the time of the northward turning, there was also the onset of a gradual ramp upward in ion flow speed at THEMIS E which at 08:03:40 sharply increased. Twenty seconds later, there was an increase in luminosity at Fort Simson (Fig. 2). Nine seconds later at 08:04:14 a fast flow burst arrived at THEMIS D. Within 3 s, a Pi 2 began at Fresno, CA, and at 08:04:47 and 08:05:05 magnetic variations began suddenly at THEMIS D and E. Since Fort Simson was in virtually the same meridian as the THEMIS spacecraft, we conclude

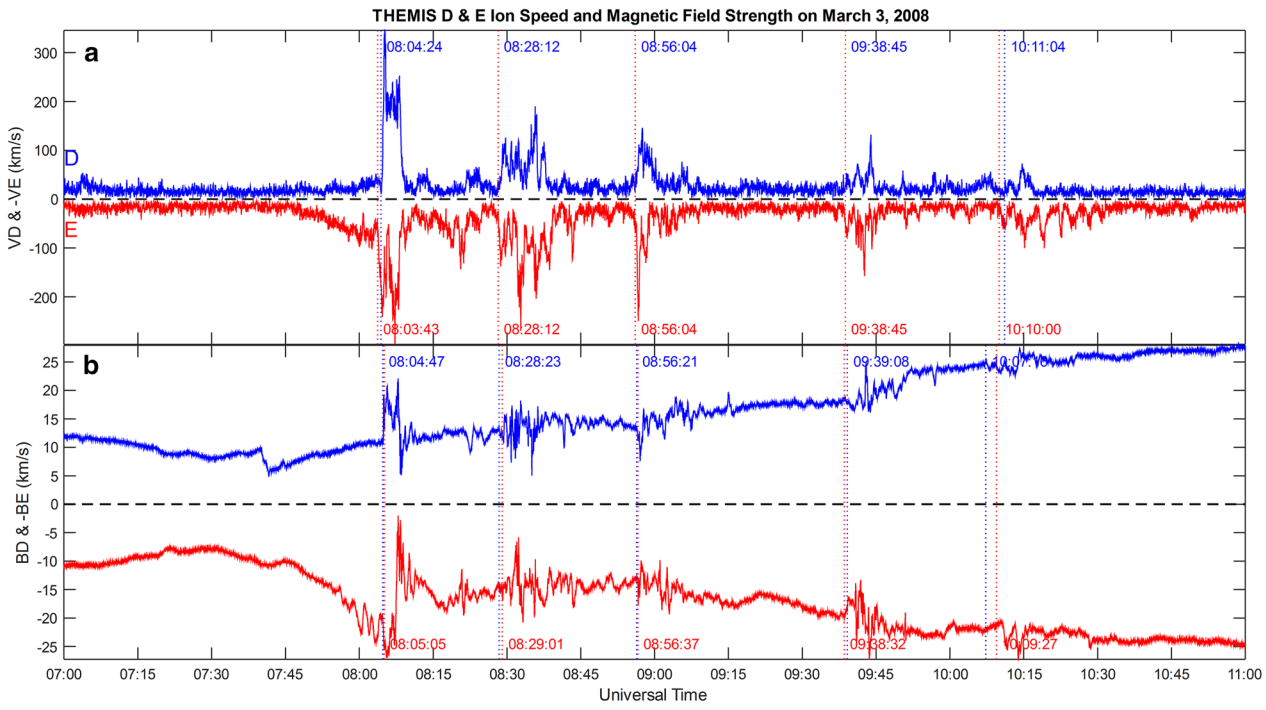

Fig. 4 Ion flow speed and magnetic field strength measured by THEMIS D and E. Panel **a** presents the ion speed at THEMIS D (*blue*) and THEMIS E (*inverted red trace*). *Vertical dotted red* and *blue lines* are the corresponding onset times measured on higher resolution *plots*. Panel **b** is a similar display for the magnitude of the magnetic field. Timing was determined on expanded plots displaying all three field components. Five flow bursts with associated magnetic fluctuations are obvious

that the flow burst caused the change in luminosity. Note, however, that the flows arrived at the two spacecraft 34 s apart and that the luminosity onset was between the two times. Also the onset of magnetic variations trailed the onset of the flows by 20 s for D and by 1 min 25 s for E. These facts indicate that the actual time difference between equatorial flow and field onsets and the auroral onset depends on the location of the spacecraft and our ability to define precise onset times. This flow burst apparently had very little effect as the weak bay ended at 08:12 and there was no Pi 2 or MPB.

A second flow perturbation not counted as a flow burst had a somewhat ambiguous onset at 08:15:21. There were minor changes in the magnetic field at the two spacecraft and minor luminosity changes at Fort Yukon and Inuvik about 2 min after the effects in space. The second major flow onset occurred simultaneously at both spacecraft at 08:27:58. Magnetic changes followed within a minute followed by a Pi 2 at 08:30:46, and then luminosity enhancements at Fort Yukon and Inuvik. Again the flow was earlier than the magnetic perturbations and both started before the luminosity enhancements. This event was associated with a rapid expansion of the plasma sheet and pulsing earthward flow as seen by THEMIS C.

The third flow burst was observed by both the D & E spacecraft at 08:56:00 with magnetic variations beginning within 40 s. The luminosity started to increase 4.5 min later at 09:00:37 and by 09:01:15, a poleward auroral expansion had begun at Inuvik. By 09:02 a negative bay in SML was in progress. The expansion and the bay ended 7 min later.

The fourth flow burst began with an event at 09:29:00 that appears to be a pseudo breakup with a small Pi 2 and small negative bay that quickly recovered. After a short delay at 09:35:45, there was a luminosity enhancement at all three stations followed by a poleward auroral expansion at Inuvik starting at 09:36:34. At 09:37 the plasma sheet expanded at THEMIS C, there was a strong earthward flow, and the field was dipoalrized. In the next 2.5 min a negative bay began, a Pi 2 started, flow bursts arrived at both THEMIS D & E, then there were enhanced magnetic variations, and finally at 09:39:00 the midlatitude positive bay started. There was an intensification of the negative bay at 09:49:00 but no other signatures. In this case, the luminosity changes were earlier than the flow bursts and magnetic field changes. We note that the peak flow velocities were weaker than the peak of all other flow bursts, but the changes in Bz were larger.

In this case, a substorm current wedge developed and the inversion indicates that the upward current was close to 20 h local time. Since the spacecraft was close to midnight, it is likely that flow bursts arrive earlier at another local time.

The fifth flow burst at 10:02:56 was the weakest of all and difficult to time at both spacecraft. There were magnetic changes at 10:07:16 and a luminosity increase at 10:09:05 far to the west at Fort Yukon. There was a short-term drop in the SML index but these changes were close to the end of the recovery phase of this substorm.

Conclusions

The event on March 3, 2008 examined here is complex exhibiting a number of the expected signatures of a substorm, but one where it is difficult to identify a single onset or three distinct phases. The AL time series shows the main event was only 2 h in duration but during this time there were at least five sudden decreases in the AL index and two incidents of poleward expansion of the aurora. The THEMIS spacecraft located just before local midnight at 11 Re shows that the interval was associated with a sequence of five fast flow bursts each transporting magnetic flux that increased the vertical magnetic field strength at the location of the spacecraft. Since there is no known explanation for fast flows carrying northward magnetic field other than reconnection, we assume that an x-line formed in the tail shortly before 08:04. THEMIS C supports this idea as the plasma sheet had thinned significantly at this time. Every flow burst was associated with intensification of the aurora at one observatory and twice with poleward expansions. In every case, the onset of the fast flow occurred before the onset of changes in the magnetic field. In all but one case the onset of the flows preceded the intensification of the aurora. Our interpretation of these observations is that fast flows are the cause of auroral intensifications but sometimes the flow arrives at a different local time than the spacecraft and later expands to include the spacecraft. During this interval, there was only one midlatitude positive bay indicating a substorm current wedge. Many investigations have used this onset as the reference time for establishing the substorm sequence. The question is why there was only one.

The midlatitude positive bay is created by the field-aligned currents (FAC) of the substorm current wedge. The only viable mechanism that has been suggested for its creation comes from the Vasyliunas equation (Vasyliunas 1970). The theory of magneto hydro dynamics (MHD) shows that there are three main sources of FAC including the inertial current created by the deceleration of flows; magnetic shear associated with field line bending due to flow shears (vorticity); and a misalignment of the gradients of plasma pressure and flux tube volume. It has been shown that the inertial current is weak and lasts only as long as the braking of the flow (Shiokawa et al. 1998). Magnetic shear depends on the strong gradients in flow velocity which are also short lived when only bursty bulk flows are present. Thus, we conclude that the misalignment of gradients is the likely driver of the substorm current wedge.

In a recently completed study, we used our list of MPB onsets (~40,000 from 1982 to 2014) to determine when the current wedge is present (Chu 2015). We then inverted most of these to determine the location and strength of the current wedge as a function of time. This information was used to locate the THEMIS spacecraft relative to the current wedge. We find that 85 % of the time plasma flows are inside the angular sector of the current wedge regardless of where it is centered. The results show a brief burst (~3 min) of high speed flow at MPB onset followed by a more gradual increase in plasma pressure and vertical magnetic field (GSM Bz). The temporal pattern of changes in ion pressure and Bz is similar to those of the wedge current and the AL index.

The formation of the substorm current wedge has been extensively studied by MHD simulations (Birn and Hesse 1991; Birn et al. 1999). As reviewed in Kepko et al. (2014), it is created by the pileup and diversion of plasma flows. As successive flows arrive in some local time sector, the plasma ahead of the flows is compressed increasing its pressure. The flows carry northward magnetic field that decreases the volume of flux tubes in the region of pileup [see Figure 4 of Kepko et al. (2014)]. In a dipole field, the pressure gradient is normally radial inward and the flux tube volume gradient is radially outward. In the pileup situation, pressure gradients point to the center of the compressed region and flux tube volume gradients point azimuthally away from the region of pileup. The misaligned gradients drive a field-aligned current system. However, the system is a quadrupole system with an outer wedge of the expected sense and an inner wedge of the opposite sense. From the ground only the difference between the two current wedges can be detected. The inner current is weaker so the difference current closes westward in the ionosphere across the auroral bulge.

Our recently completed studies indicate one change should be made to this picture. The plasma in the pileup region has higher pressure than the surroundings so that a ridge of high pressure is built outward into the tail. The gradients still drive a quadrupole current system with the outer system dominant. In the example reported here, the first three flow bursts did not create an observable current wedge but the arrival of the fourth did. We

suggest that it may often take more than one flow burst to establish the proper distributions of pressure and flux tube volume to create a substorm current wedge. Once the current wedge begins to grow, it alters the configuration of the magnetic field and hence the mapping of a fixed point in the equatorial plane. Elsewhere we have shown (Chu et al. 2015b) that dipolarization of the field causes the footprint of a fixed point to move poleward. Combined with the outward growth of the pileup region, one can explain the expansion of the aurora in conjunction with the presence of the current wedge.

Additional files

Additional file 1: Figure S1. Auroral luminosity on a north–south meridian over Fort Simson as function of time. Keogram for Fort Simson, NWT, Canada. The vertical axis shows magnetic latitude along a magnetic north–south meridian of an image focused by a fish eye lens on a 256 by 256 sensor array. The horizontal axis is universal time and the color scale shows the intensity of light at different zenith angles. Vertical dashed lines are times of the onset of fast flows at THEMIS spacecraft.

Additional file 2: Figure S2. Auroral luminosity on a north–south meridian over Inuvik as function of time. Keogram for Inuvik, NWT, Canada for the interval 08-10 UT is shown. Two poleward expansion of aurora are seen after 09:01:15 and 09:36:34 UT.

Additional file 3: Figure S3. Auroral luminosity on a north–south meridian over Fort Yukon as function of time. Keogram for Fort Yukon, NWT, Canada for the interval 08-10 UT is shown. Intense aurora was observed in association with fast flows at 08:56 and 09:38 UT. The first at 09:01:42 caused a poleward expansion. The next two appear to be effects of surges moving westward over the station.

Additional file 4: File 1. Mosaic map projection of aurora over northwestern North America. This zip archive contains 2401 gif images presenting the time development of the aurora over the western part of Canada and Alaska at a 3.0 s cadence. The all sky image data have been transformed to magnetic coordinates and projected onto a map.

Additional file 5: Figure S4. The orbits of Themis C (blue), THEMIS D (red), THEMIS E (black), and GOES 11 (black) are plotted from 7 to 11 UT. Horizontal triangles show times of flow bursts recorded at THEMIS D & E. The marker "X" denotes the start of hourly intervals. A blue dashed line indicates the center of the downward current at expansion onset and red the center of the upward current.

Additional file 6: Figure S5. Components of the GSM magnetic field at the THEMIS D spacecraft. Time series of the X, Y, Z components of the magnetic field at THEMIS D are plotted in GSM coordinates. Vertical dotted lines are the times of onset of the magnetic perturbations associated with ion flow bursts. Each flow burst is associated with an increase in Bz and fluctuations in all components.

Additional file 7: Figure S6. Components of the GSM magnetic field at the THEMIS E spacecraft. Same as Additional file 6: Figure S5 for the THEMIS E spacecraft.

Additional file 8: Figure S7. Observations at THEMIS C on March 3, 2008. Panel (a) displays the thermal pressure of ions, the magnetic pressure, and their sum. Panel (b) presents the speed of ions. Vertical dotted lines are the time of flow onsets observed closer to the Earth by either THEMIS D or E.

Additional file 9: Table S1. The time sequence of events observed in different substorm indicators. The table contains a chronological list of distinct events identified in different indicators of substorm activity. Time is given in the format HHMMSS.

Abbreviations

AL: auroral lower; ASI: all sky imager; Bi: component of the magnetic field; FAC: field-aligned current; GOES: geosynchronous operational environmental satellite; GSM: geocentric solar magnetospheric; H: horizontal component; Hp: field component parallel to rotation axis; IMF: interplanetary magnetic field; MHD: magnetohydrodynamics; MPB: midlatitude positive bay; Pi 2: pulsation irregular type 2; SCW: substorm current wedge; SML: supermag AL index; THEMIS: time history of events and macroscale interactions during substorms; UT: universal time; UCF: universal coupling functions.

Authors' information

RM was the creator of the concept of the substorm current wedge and one of the originators of the concept of a magnetospheric substorm. He helped develop the original near-Earth neutral line model which posits that the substorm is caused by magnetic reconnection in the tail. He is an advocate of the idea that the auroral expansion is a consequence of the pileup of plasma and magnetic field carried earthward by reconnection driven flows. XC has been a graduate student supervised by RM. He invented the MPB index and revitalized the numerical model of the current wedge. His statistical investigation of spacecraft data has led to the conclusions described in this paper.

Authors' contributions

RM was invited to prepare a historical review of auroral substorms and the substorm current wedge. XC created the MPB index and performed the data inversions to obtain the current wedge parameters shown in this paper. XC completed his Ph.D. dissertation investigating the formation of the current wedge using spacecraft data. The interpretation of wedge formation presented in this paper is the primary conclusion of his dissertation. RM analyzed the THEMIS data and prepared all of the figures used in this paper. He also wrote the initial manuscript. Both authors read and approved the final manuscript.

Acknowledgements

This work has been supported by numerous NASA and NSF grants over many years. Specifically, this paper was funded by NSF GEM 1003854 and NASA NESSF NNX14AO02H. We gratefully acknowledge THEMIS (themis. ssl.berkeley. edu), INTERMAGNET (http://www.intermagnet.org)), GOES, OMNI database (omniweb.gsfc.nasa.gov), SuperMAG (supermag.jhuapl.edu), and their data providers. The authors would also like to thank the NASA NSSDC and NASA VMO centers.

Competing interests

The authors declare that they have no competing interests.

Received: 30 December 2015 Accepted: 20 March 2016
Published online: 12 April 2016

References

Akasofu S-I (1964) The development of the auroral substorm. Planet Space Sci 12(4):273–282

Akasofu S-I, Chapman S (1963a) The development of the main phase of magnetic storms. J Geophys Res 68(1):125–129. doi:10.1029/JZ068i001p00125

Akasofu SI, Chapman S (1963b) Magnetic storms—simultaneous development of main phase (Dr) and of polar magnetic substorms (Dp). J Geophys Res 68(10):3155. doi:10.1029/JZ068i010p03155

Akasofu SI, Meng CI (1969) A study of polar magnetic substorms. J Geophys Res 74(1):293. doi:10.1029/JA074i001p00293

Akasofu S-I, Chapman S, Venkatesan D (1963) The main phase of great magnetic storms. J Geophys Res 68(11):3345–3350. doi:10.1029/JZ068i011p03345

Akasofu S-I, Chapman S, Meng CI (1965) The polar electrojet. J Atmos Terr Phys 27(11/12):1275–1305. doi:10.1016/0021-9169(65)90087-5

Birn J, Hesse M (1991) The substorm current wedge and field-aligned currents in mhd simulations of magnetotail reconnection. J Geophys Res 96(A2):1611–1618. doi:10.1029/90JA01762

Birn J, Hesse M, Haerendel G, Baumjohann W, Shiokawa K (1999) Flow braking and the substorm current wedge. J Geophys Res 104(A9):19895–19903. doi:10.1029/1999JA900173

Brice N (1967) Morphology of elementary magnetospheric substorms. Sydney, ESSA Tech Mem IERTM-ITSA, 72

Chapman S (1962) Earth storms: retrospect and prospect. J Phys Soc Jpn 17(A-I):6

Chu X (2015) Configuration and generation of substorm current wedge. University of California Los angeles, Los Angeles

Chu XN, Hsu TS, McPherron RL, Angelopoulos V, Pu ZY, Weygand JJ, Khurana K, Connors M, Kissinger J, Zhang H, Amm O (2014) Development and validation of inversion technique for substorm current wedge using ground magnetic field data. J Geophysical Res-Space Phys 119(3):1909–1924. doi :10.1002/2013ja019185

Chu X, McPherron RL, Hsu T-S, Angelopoulos V (2015a) Solar cycle dependence of substorm occurrence and duration: implications for onset. J Geophysical Res-Space Phys 120(4):2808–2818. doi:10.1002/2015ja021104

Chu X, McPherron RL, Hsu T-S, Angelopoulos V, Pu Z, Yao Z, Zhang H, Connors M (2015b) Magnetic mapping effects of substorm currents leading to auroral poleward expansion and equatorward retreat. J Geophysical Res-Space Phys 120(1):253–265. doi:10.1002/2014ja020596

Coroniti F, McPherron R, Parks G (1968) Studies of the magnetospheric substorm, 3, concept of the magnetospheric substorm and its relation to electron precipitation and micropulsations. J Geophys Res 73(5):1715–1722. doi:10.1029/JA073i005p01715

Cowley SWH (1982) Substorms and the growth phase problem. Nature 295(4):365–366

de la Beaujardiere O, Lyons LR, Friis-Christensen E (1991) Sondrestrom radar measurements of the reconnection electric field. J Geophys Res 96(A8):13907–13912. doi:10.1029/91JA01174

De La Beaujardiere O, Lyons LR, Ruohomemi JM, Friss-Christensen E, Danielsen C, Rich F, Newell P (1994) Quiet-time intensifications along the poleward auroral boundary near midnight. J Geophys Res 99(A1):287–298. doi:10.1029/93JA01947

Fukushima N, Kamide Y (1973) Contribution Of Magnetospheric field-aligned current to geomagnetic bays and sq fields—comment on partial ring-current models. Radio Sci 8(11):1013–1017. doi:10.1029/RS008i011p01013

Horning B, McPherron R, Jackson D (1974) Application of linear inverse theory to a line current model of substorm current systems. J Geophys Res 79(34):5202–5210. doi:10.1029/JA079i034p05202

Jelly D, Brice N (1967) Changes In van allen radiation associated with polar substorms. J Geophys Res 72(23):5919–5931

Kepko L, McPherron RL, Amm O, Apatenkov S, Baumjohann W, Birn J, Lester M, Nakamura R, Pulkkinen TI, Sergeev V (2014) Substorm current wedge revisited. Space Sci Rev 190:1–46. doi:10.1007/s11214-014-0124-9

Lyons L, Nagai T, Blanchard G, Samson J, Yamamoto T, Mukai T, Nishida A, Kokubun S (1999) Association between Geotail plasma flows and auroral poleward boundary intensifications observed by CANOPUS photometers. J Geophys Res 104(A3):4485–4500. doi:10.1029/1998JA900140

McPherron, R.L., G.K. Parks, and F. Coroniti (1967) Relation of correlated magnetic micropulsations and electron precipitation to the auroral substorm, In Proceedings of the conjugate point symposium, ITSA Mem. 72, Boulder, Colorado

McPherron R (1970) Growth phase of magnetospheric substorms. J Geophys Res 75(28):5592–5599. doi:10.1029/JA075i028p05592

McPherron RL (1972) Substorm related changes in the geomagnetic tail: the growth phase. Planet Space Sci 20(9):1521–1539

McPherron R, Parks G, Coroniti F, Ward S (1968) Studies of the magnetospheric substorm, 2, correlated magnetic micropulsations and electron precipitation occurring during auroral substorms. J Geophys Res 73(5):1697–1713. doi:10.1029/JA073i005p01697

McPherron RL, Russell CT, Aubry M (1973) Satellite studies of magnetospheric substorms on August 15, 1968, 9. Phenomenological model for substorms. J Geophys Res 78(16):3131–3149

McPherron RL, Hsu T-S, Chu X (2015) An optimum solar wind coupling function for the AL index. J Geophysical Res-Space Phys 120(4):2494–2515. doi:10.1002/2014ja020619

Mozer F (1973) On the relationship between the growth and expansion phases of substorms and magnetospheric convection. J Geophys Res 78(10):1719–1722. doi:10.1029/JA078i010p01719

Newell PT, Gjerloev JW (2011) Evaluation of SuperMAG auroral electrojet indices as indicators of substorms and auroral power. J Geophysical Res-Space Physics 116:A12. doi:10.1029/2011ja016779

Parks G, Coroniti F, McPherron R, Anderson K (1968) Studies of the magnetospheric substorm 1 characteristics of modulated energetic electron precipitation occurring during auroral substorms. J Geophys Res 73(5):1685–1696. doi:10.1029/JA073i005p01685

Rostoker G, Akasofu S-I, Foster J, Greenwald R, Kamide Y, Kawasaki K, Lui A, McPherron R, Russell C (1980) Magnetospheric substorms & mdash;definition and signatures. J Geophys Res 85(A4):1663–1668. doi:10.1029/JA085iA04p01663

Rostoker G, Akasofu SI, Baumjohann W, Kamide Y, McPherron RL (1987) The roles of direct input of energy from the solar wind and unloading of stored magnetotail energy in driving magnetospheric substorms. Space Sci Rev 46(1–2):93–111

Sergeev V, Liou K, Meng C-I, Newell P, Brittnacher M, Parks G, Reeves G (1999) Development of auroral streamers in association with localized impulsive injections to the inner magnetotail. Geophys Res Lett 26(3):417–420. doi:10.1029/1998GL900311

Shiokawa K, Baumjohann W, Haerendel G, Paschmann G, Fennell JF, Friis-Christensen E, Luhr H, Reeves GD, Russell CT, Sutcliffe PR, Takahashi K (1998) High-speed ion flow, substorm current wedge, and multiple Pi 2 pulsations. J Geophysical Res-Space Phys 103(A3):4491–4507. doi:10.1029/97ja01680

Vasyliunas VM (1970) Mathematical models of magnetospheric convection and its coupling to the ionosphere, particles and fields in the magnetosphere, 60–71

Vasyliunas VM, Wolf RA (1973) Magnetospheric substorms—some problems and controversies. Rev Geophys 11(1):181–189. doi:10.1029/RG011i001p00181